MULTI-PARAMETER HOMOTOPY METHODS FOR FINDING DC OPERATING POINTS OF NONLINEAR CIRCUITS

by

Denise M. Wolf and Seth R. Sanders

Memorandum No. UCB/ERL M95/86

1 August 1995

MULTI-PARAMETER HOMOTOPY METHODS FOR FINDING DC OPERATING POINTS OF NONLINEAR CIRCUITS

by

Denise M. Wolf and Seth R. Sanders

Memorandum No. UCB/ERL M95/86

1 August 1995

ELECTRONICS RESEARCH LABORATORY

College of Engineering
University of California, Berkeley
94720

Multi-Parameter Homotopy Methods For Finding DC Operating Points of Nonlinear Circuits *

Denise M. Wolf and Seth R. Sanders

Department of Electrical Engineering and Computer Sciences
University of California, Berkeley CA 94720
e-mail: dwolf@eecs.berkeley.edu and sanders@eecs.berkeley.edu

Abstract

This paper introduces real and complex multi-parameter homotopy methods for finding DC solutions of nonlinear circuits. We show, using arguments from algebraic geometry, that multi-parameter homotopy methods can avoid folds and bifurcation points along solution paths, and can find multiple solutions. Examples based on polynomial equations and circuits are used to illustrate the concepts.

1 Introduction

Calculating the DC operating points of nonlinear circuits and systems is a difficult task requiring the solution of nonlinear algebraic equations. Most circuit simulators use the Newton-Raphson method or one of its variants to calculate DC operating points. While these methods are robust and quadratically convergent if a starting point sufficiently close to a solution is supplied, they may fail if no such point is known.

Continuation and probability-1 homotopy methods, with their potentially large or global regions of convergence, have been used to solve circuit equations [4, 5, 7]. The idea behind a continuation method is to embed a parameter in the circuit's nonlinear equations. Setting the parameter to zero reduces the problem to a simple one that can be solved easily, or whose solution is known. The solution to the simple problem is the starting point of a continuation path. The set of equations is then continuously deformed into the originally-posed difficult problem by varying the embedded parameter from zero to the required final value.

Continuation methods may suffer from a variety of ills, including the presence of bifurcations and sharp folds (turning points) along solution paths, infinite solutions, abbreviated

*This work was supported by SRC contract 93-DC-324, and grants from Tandem Computers and the UC Micro Program.

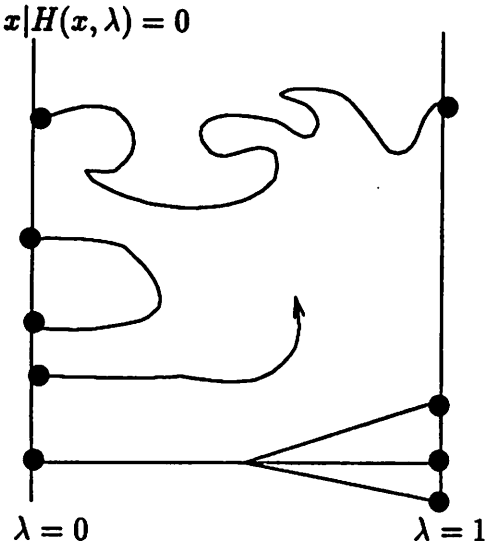

Figure 1: Folding, abbreviated, divergent, and bifurcating homotopy solution paths.

paths, closely spaced solution curves, and disconnected branches [8]. Some of these possibilities are illustrated in Figure 1. Closely spaced curves may lead to curve jumping, and disconnected branches are problematic for methods that follow extended curves to find multiple solutions [5].

Probability-1 convergent homotopy methods guarantee, with the satisfaction of a coercivity condition, a bifurcation-free path with finite arc length to a simple solution for almost all initial values (see [8] and references therein). However, the coercivity condition may not always be satisfied, and the problem of finding multiple operating points is not addressed.

In this paper we introduce the concept of real and complex multi-parameter homotopy maps and methods for solving nonlinear circuits. We explore their potential for avoiding folds and fork bifurcations along solution paths, and for finding all circuit solutions. We illustrate these concepts on polynomial and circuit examples. Simple, isolated solution points in a compact region are assumed.

2 Multi-Parameter Maps and Methods

Standard homotopy functions, which we will refer to as single parameter homotopies, are a special case of multi-parameter homotopies. A typical single parameter homotopy function used to solve $f(x)=0, f:\Re^n \rightarrow \Re^n$, is

$$H(x,\lambda)=(\lambda)f(x)+(1-\lambda)g(x),\ \lambda\in[0,1]. \tag{1}$$

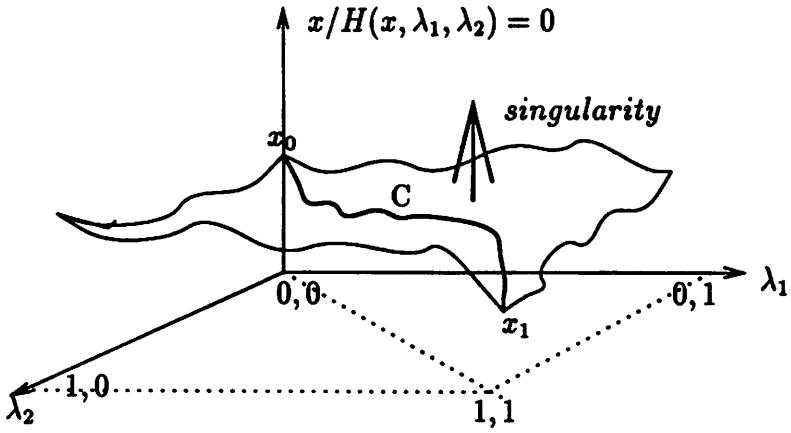

Figure 2: *Expand dimensionality* of homotopy function and try to forge better paths across solution space from x_0 to x_1.

Embedding f into H, a function with one added parameter and the starter system $g(x) = 0$, transforms the solution set of $f(x) = 0$ from isolated points in $\Re^n$ to a set of curves in $\Re^n \times [0,1]$, the characteristics of which will influence the efficiency of any curve tracing algorithm. If, for example, the solution curves are long, circuitous and/or ill-conditioned, the algorithm may be inefficient or may not converge.

Two examples of 2-parameter homotopy functions are

$$H(x,\lambda_1,\lambda_2) = (\lambda_1)f(x) + (1-\lambda_2)g(x),\ \lambda_1,\ \lambda_2 \in \Re, \tag{2}$$

and

$$H(x,\lambda) = (\lambda)f(x) + (1-\lambda)g(x),\ \lambda \in C. \tag{3}$$

The first is an example of a *real 2-parameter homotopy map* and the second of a *complex parameter homotopy map.* In the latter, the two parameters are the real and imaginary parts of λ. In the case of complex parameter homotopy, we assume that the resulting function H is well defined for complex x and λ, specifically that H has a useful region of *analyticity* in C^n x C. A function $H(x,\lambda)$, $h : C^n \times C \rightarrow C$, is *analytic* if it has a local power series expansion in all variables.

In these cases, embedding f into H, a function with two parameters, transforms the solution set of $f(x) = 0$ from a set of isolated points to locally 2-d *surfaces.* See Figure 2 for an illustration. Since the solution set is composed of surfaces rather than curves, there are (if any) *infinitely many solution paths* passing from the solutions of the initial, simple problem $g(x) = 0$ at $\lambda_1 = \lambda_2 = 0$ ($\lambda_r = \lambda_i = 0$) to the solutions of the final, hard problem $f(x) = 0$ at $\lambda_1 = \lambda_2 = 1$ ($\lambda_r = 1, \lambda_i = 0$). This lack of uniqueness opens up the possibility of forging paths over the solution surfaces that may be better than the solution curves produced by the corresponding single parameter homotopy, as well as relaxing the conditions on homotopy

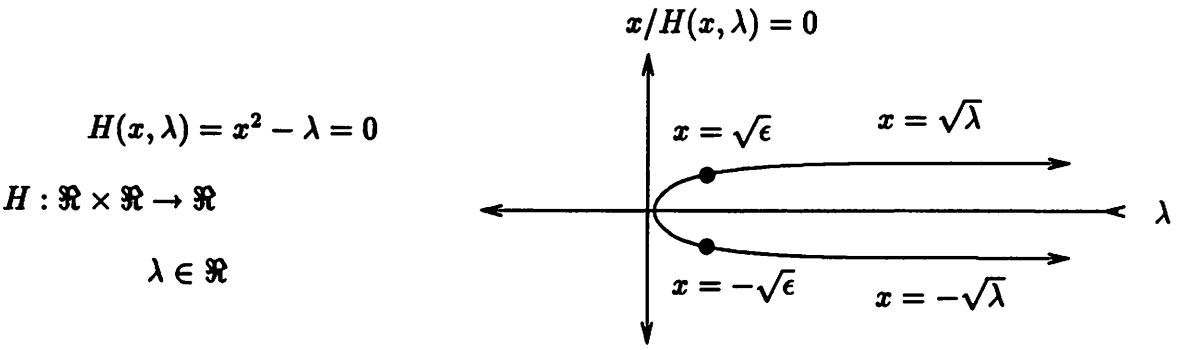

Figure 3: Example of a fold.

functions that guarantee smooth non-intersecting paths to solution points. Thus, an ideal multi-parameter homotopy method is an algorithm capable of forging paths on solution surfaces from the initial parameter vector λ_0 to the final parameter vector λ_f that are as short and smooth as possible, and that avoid singularities and any other point and curve features deemed undesirable.

The following two sections begin to answer the question of which 'bad' point and curve features may be avoided by employing real multi-parameter homotopies or complex multi-parameter homotopies. Specifically, Section 3 deals with folds along solution paths, while Section 4 addresses bifurcations. These sections also outline some necessary features of algorithms capable of avoiding such obstacles. Section 5 outlines the potential for finding multiple solutions of a given circuit or system of algebraic equations via complex multi-parameter homotopy.

3 Avoiding Folds

A folding solution path associated with a real 1-parameter homotopy function $H(x,\lambda)=0$ ($H:\Re^n\times L\to\Re^n, L\subset\Re$) reverses direction along the parameter axis. Although a fold can correspond to a repeated root of multiplicity greater than two, generic folds correspond to real *double roots*, occurring at parameter values we refer to as *generic fold values*. At a solution corresponding to a generic fold value, the Jacobian matrix $DH_x(x,\lambda)$ drops rank, while the extended Jacobian matrix $DH_{x,\lambda}(x,\lambda)$ maintains rank. Note that DH_x indicates the Jacobian matrix $\partial H/\partial x$ with λ acting as a parameter. The term $DH_{x,\lambda}(x,\lambda)$ refers to the extended Jacobian matrix $[\partial H/\partial x, \partial H/\partial\lambda]$, with λ treated as an additional variable.

In the present paper, we deal only with singular points where the matrix DH_x drops rank exactly once. In this case, Lyapunov-Schmidt reduction, as discussed in [13] and summarized in Appendix A, can be applied to develop a scalar equation locally characterizing the singularity. In our discussions, we take advantage of this fact by analyzing scalar equations to develop intuition that is then applied to multivariate systems of equations.

The simplest example of a solution curve with a fold, or turning point, is shown in Figure 3. At the critical fold value $\lambda = 0$ of the homotopy function $H(x, \lambda) = x^2 - \lambda = 0$, two real solution branches $x^+ = +\sqrt{\lambda}$ and $x^- = -\sqrt{\lambda}$ coalesce into a real double-root. Figures 9 and 11 illustrate further examples of solution curves with folds that, though arising from more complicated equations, are locally equivalent to the simple quadratic example.

Single-parameter homotopy methods capable of handling solution curves with folds, such as those in Figures 3, 9, and 11, must be able to respond by reversing direction along the parameter axis. This maneuver can be inefficient for arc length parameterized methods such as those in [8] because of the small step sizes required to make these turns. While faster than the above mentioned methods, switched parameter algorithms [5] may miss sharp turning points if the step size is not small enough, and can exhibit cyclic behavior near switching points. In this section, we explore the potential of real and complex multi-parameter homotopy methods for avoiding folds, and indicate how this avoidance, when possible, may be accomplished. We show:

Result 1: Real multi-parameter methods generally *cannot* avoid folds along solution curves without passing through a singular point, corresponding to a repeated root of order two or greater.

Result 2: Complex parameter methods *can* avoid folds along solution curves. Generic folds may be avoided by tracing a closed curve in complex parameter space around the parameter value corresponding to the fold.

Results 1 and 2 may be explained by considering the codimension of bifurcation sets in real and complex parameter space. For a system of parameterized nonlinear equations $H(x, \bar{\lambda}) = 0$, the *bifurcation set* B consists of parameter vectors $\bar{\lambda}$ for which the system of equations has repeated roots. Here, the overbar notation $(\bar{\lambda})$ denotes a parameter vector. A *regular* value is the term used to describe a parameter vector that does not result in repeated roots, and hence does not belong to the bifurcation set.

A value $\bar{\lambda}_b$ in the *bifurcation set* B is characterized by the existence of an x_b satisfying

$$H(x_b, \bar{\lambda}_b) = 0 \tag{4}$$

$$rank(DH_x(x_b, \bar{\lambda}_b)) < n \tag{5}$$

Since generic fold values are parameter values at which a homotopy function has a real double root, generic fold values belong to the bifurcation set. Thus, bifurcation set properties are intimately linked to the potential for fold avoidance in real and complex parameter spaces.

Figure 4 illustrates the codimension of bifurcation sets in real and complex parameter space. A bifurcation set in *real* parameter space has *codimension one* and *divides* the parameter space. If a set may be described by a single constraint on a larger space (say $\Re^n$), then it has codimension one with respect to that space. For instance, a curve has codimension one within a plane (as shown in Figure 4(a)), and a locally 2-d surface has codimension one

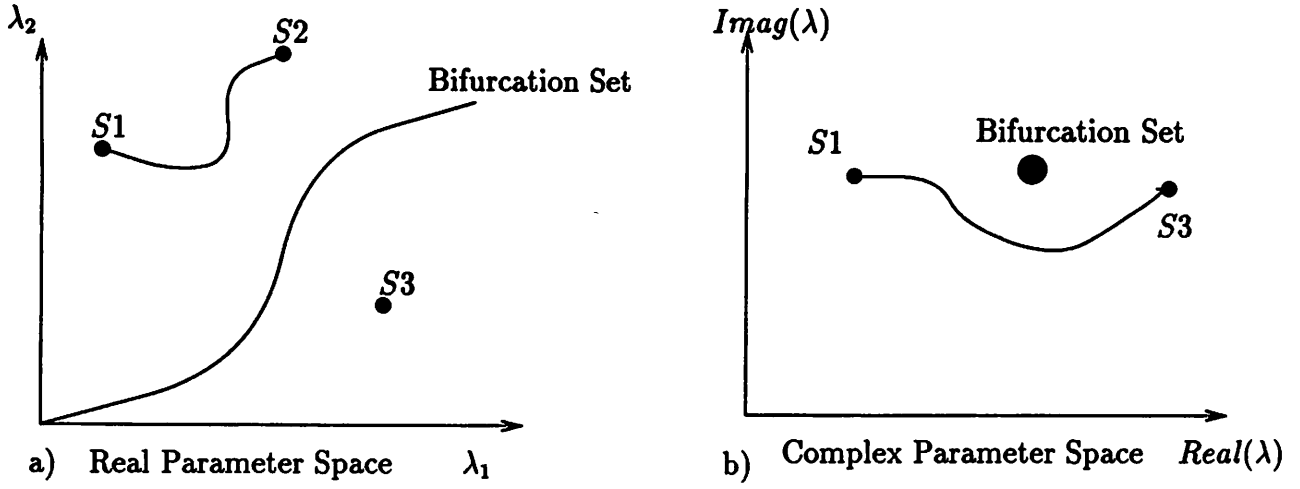

Figure 4: a)Bifurcation set of codimension-1 in real parameter space. b) Bifurcation set of codimension-2 in complex parameter space.

within $\Re^3$. As a specific example, the bifurcation set of the real-coefficient quadratic equation $x^2 + \lambda_1 x + \lambda_2 = 0$ has codimension one since it is described by the curve $\lambda_1^2 - 4\lambda_2 = 0$ in $\Re^2$.

In complex parameter space, the bifurcation set has *codimension two* and *does not divide* the parameter space. If a set may be described by two constraints on a larger space, it has codimension two with respect to that space. For example, a point within a plane has codimension two (shown in Figure 4(b)), as does a curve within $\Re^3$. The complex-coefficient quadratic $H(x, \lambda) = x^2 + \lambda = 0$ ($\lambda \in C$), for instance, has the bifurcation set $\lambda = 0$, a *point* within the complex parameter *plane*.

To see why bifurcation sets in real parameter space have codimension one and and those in complex parameter space have codimension two, consider equations (4) and (5), used to characterize the bifurcation set. In the real case we have the n equations $H(x, \bar{\lambda}) = 0$ plus the scalar real equation $\det(DH_x(x, \bar{\lambda})) = 0$. Hence, the implicit function theorem may be applied to derive a single equation that locally describes the codimension one bifurcation set (one constraint in parameter space). [1] In contrast, equation (5) imposes two constraints in the complex case, $\mathrm{Re}(\det(DH_x(x, \lambda_b))) = 0$ and $\mathrm{Im}(\det(DH_x(x, \lambda_b))) = 0$, which leads to

[1] Recall that the implicit function theorem [19] implies that, given a continuously differentiable function $F : \Re^n \times \Re^m \rightarrow \Re^n$ and a point $(x_0, \bar{\lambda}_0) \in \Re^n \times \Re^m$ such that the Jacobian $DF_x(x_0, \bar{\lambda}_0)$ is full rank, then there exists an open neighborhood of $(x_0, \bar{\lambda}_0)$ and a unique function g over which $x = g(\bar{\lambda})$. Applying this theorem to a collection of n equations consisting of $n-1$ of the n equations $H(x, \bar{\lambda}) = 0$, plus the equation $\det(DH_x(x, \bar{\lambda})) = 0$, at points $(x_b, \bar{\lambda}_b)$ where the rank of the Jacobian of the n assembled equations is full, allows x to be expressed as $x = g(\bar{\lambda})$ over a neighborhood of $(x_b, \bar{\lambda}_b)$. One may then substitute the function $x = g(\bar{\lambda})$ into the remaining equation of $H(x, \bar{\lambda}) = 0$ to get an equation $h_i(g(\bar{\lambda}), \bar{\lambda}) = 0$ locally describing the bifurcation set of H.

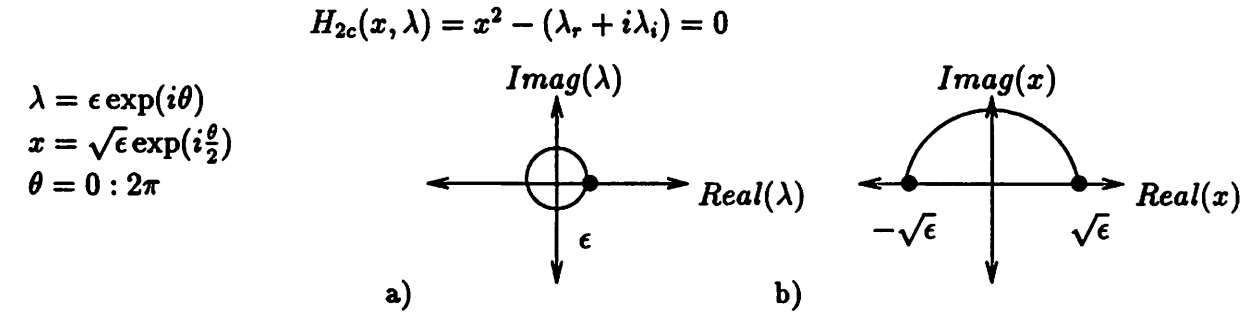

Figure 5: Complex 2-parameter homotopy for fold avoidance. a) A 2π rotation in complex parameter space around the critical fold value. b) The complex, regular solution path (fold-free) corresponding to the complex parameter excursion shown in (a).

the derivation of a codimension two bifurcation set by application of the implicit function theorem.

In a parameter space with a codimension one bifurcation set, it is in general *not* possible to trace a continuous path from one arbitrarily chosen point to another without passing through the bifurcation set. If, for instance, one wants to trace a continuous path from system $S1$ to system $S3$ in Figure 4(a), this path must pass through the bifurcation set B. Since generic fold values belong to a codimension one bifurcation set with respect to real parameter space, embedding additional real parameters in a homotopy function with folding solution paths cannot, in general, lead to the possibility of paths through parameter space that do not intersect the bifurcation set, which includes generic fold values and singular points corresponding to repeated roots of multiplicity greater than two.

In a parameter space with a codimension two bifurcation set, it *is* possible to trace a continuous path from any arbitrarily chosen *regular* point to any other without passing through the bifurcation set, as shown in Figure 4(b). Generic fold values belong to a codimension two bifurcation set with respect to complex parameter space. Thus, generic fold values associated with real 1-parameter homotopy functions may be avoided by complexification of the homotopy parameter λ and maneuvering through the complex parameter plane. As discussed above, the corresponding solution path also becomes complex for the complex parameter λ.

In summary, the codimension of bifurcation sets in real and complex parameter space has the very important implication that given a real homotopy function H with folding solution paths, there is a continuous path in complex parameter space from an initial 'easy' system $H(x, \lambda_0) = 0$ to the final 'hard' system $H(x, \lambda_f) = F(x) = 0$ that does not pass through the bifurcation set. This is not true in real space. Results 1 and 2 are based on these properties.

Application: Avoiding Folds with Complex Parameter Homotopy We now move on to fold-avoidance in complex space. As stated in Result 2, folds along solution curves

may generally be avoided by tracing a closed curve (2π rotation) in complex parameter space around the parameter value corresponding to the fold. To illustrate, consider the quadratic equation $H(x,\lambda) = x^2 - \lambda = 0$, which, for varying $\lambda \geq 0$, describes a generic fold with turning point $\lambda = 0$ (see Figure 3). If we want to pass from $x = \sqrt{\epsilon}$ on the solution manifold $x = \sqrt{\lambda}$ to $x = -\sqrt{\epsilon}$ on the solution manifold $x = -\sqrt{\lambda}$ without encountering a turning point, we may make λ complex and trace the curve $\lambda = \epsilon e^{i\theta}$ in parameter space from $\theta = 0$ to $\theta = 2\pi$ (see Figure 5(a)). This full circle traces the solution $x = \sqrt{\epsilon}e^{i\frac{\theta}{2}}$ from $\sqrt{\epsilon}$ to $-\sqrt{\epsilon}$ along a smooth, fold free path (see Figure 5(b)). More generally, if a generic fold (locally representable by a scalar quadratic via Lyapunov-Schmidt reduction, as discussed in Appendix A) is encountered while tracing a real homotopy path, then there exists a starting value λ^*, a radius r, and a direction $d \in \{-1, 1\}$, such that the traversal of a full circle in complex parameter space $\lambda = \lambda^* + dr(1 - e^{i\theta}), \theta = 0 : 2\pi$, will result in a fold- and bifurcation-free path around the generic fold value. In the quadratic example, $H(x,\lambda) = x^2 - \lambda = 0$, the path being traced toward the fold point is along decreasing λ, so $d = -1$. As noted previously, at a generic fold value the matrices DH_x and $DH_{x,\lambda}$ drop and maintain rank, respectively, so their conditioning may be used as a local test to indicate the approach to a fold.

A larger context for understanding fold avoidance in complex space may be found in algebraic geometry [10], as follows. A key result in this field is that an ordinary branch point, a (possibly) complex-valued parameter value corresponding to a repeated root of multiplicity n, must be circled n times in complex space in order to return to the orginal solution manifold. Each revolution has the effect of moving the solution point from one solution manifold to another (there are n), until the nth revolution returns the solution point to the original manifold. This local solution structure of n connected sheets is called an algebraic element of order $n - 1$.

A generic fold in real parameter space is an algebraic element of order one, with a repeated root of multiplicity two. A fold that does not correspond to a repeated root of multiplicity two may be associated with a higher order algebraic element. In this case, the Hessian matrix DH_{xx} will drop rank, along with DH_x. For a fold corresponding to a repeated root of multiplicity n, locally representable by a change of coordinates to the form $x^n - \lambda = 0$, $\frac{n}{2}$ revolutions in complex parameter space will result in fold avoidance and a return to a real solution branch. For example, consider the polynomial system $x^4 - \lambda = 0$, which has four repeated roots at $\lambda = 0$ with two real solution branches. In order to pass from $x = \epsilon^{1/4}$ to $x = -\epsilon^{1/4}$ (around the fold value $\lambda = 0$), two revolutions in complex parameter space are required. In the case of a transcendental singularity, an infinite number of solution branches may exist, so that no finite number of revolutions will return the solution trajectory to a real branch.

Next, we present fold-avoidance on an example circuit, and on the example homotopy function $H(x,\lambda) = sin(1/x) - \lambda$. Our simulation results indicate that the efficiency of fold avoidance in complex space is relatively independent of fold sharpness.

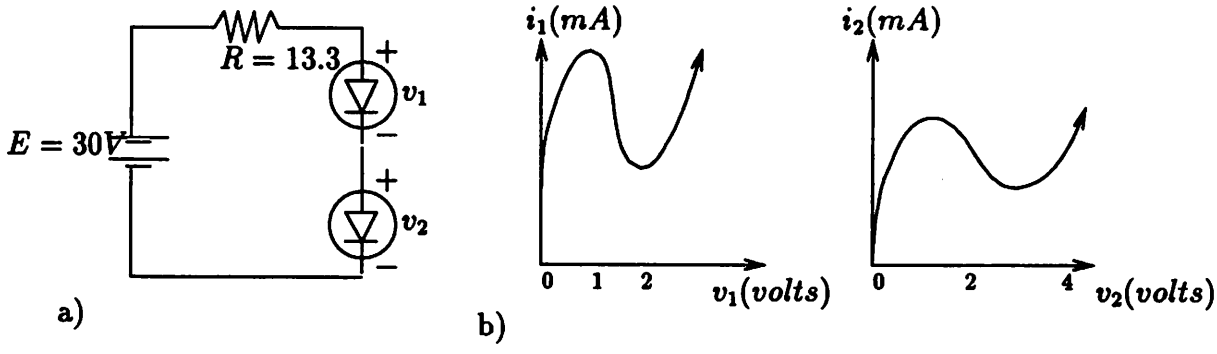

Figure 6: a) Tunnel diode circuit b) Diode characteristics.

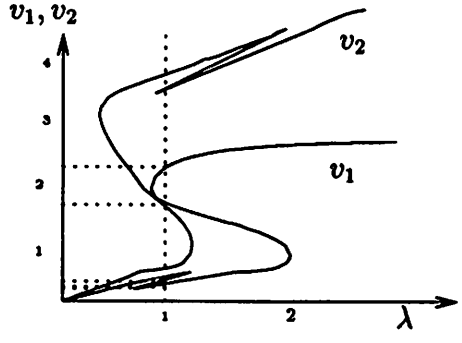

Figure 7: Drawing of real solution curve with folds for the tunnel diode circuit, passing through five solutions $v = (v_1, v_2)$, at $\lambda = 1$.

Example 1 (Tunnel Diode Circuit):

The tunnel diode circuit in Figure 8 (from [5]) has operating points determined by the loop equation $f_1(v) = E - Rg_1(v_1) - (v_1 + v_2) = 0$ and node equation $f_2(v) = g_1(v_1) - g_2(v_2) = 0$, with $v = (v_1, v_2)$. The tunnel diode currents are given by $i_1 = g_1(v_1) = 2.5v_1^3 - 10.5v_1^2 + 11.8v_1$ and $i_2 = g_2(v_2) = 0.43v_2^3 - 2.69v_2^2 + 4.56v_2$. The real 1-parameter homotopy function used in [5] is

$$\begin{aligned} H_1(v, \lambda) &= f_1(v) + (\lambda - 1)f_1(v_0) \\ H_2(v, \lambda) &= f_2(v) + (\lambda - 1)f_2(v_0) \end{aligned}$$

with $\lambda, v_1, v_2 \in \Re$. At $\lambda = 0$, a solution to $H(v, \lambda) = 0$ is $v = v_0$, which serves as a starting value for the continuation path. Figure 9 shows a real folding solution path emerging from $v_0 = (0, 0)$. Critical fold values occur at around $\lambda \approx 0.8, 1.2$ and 2.1.

We obtain a complex parameter homotopy function from the single parameter function defined in [5] by complexification ($\lambda = \lambda_r + i\lambda_i$). Now $H' : C^2 \times C \rightarrow C^2$. The real representation of these equations is as follows.

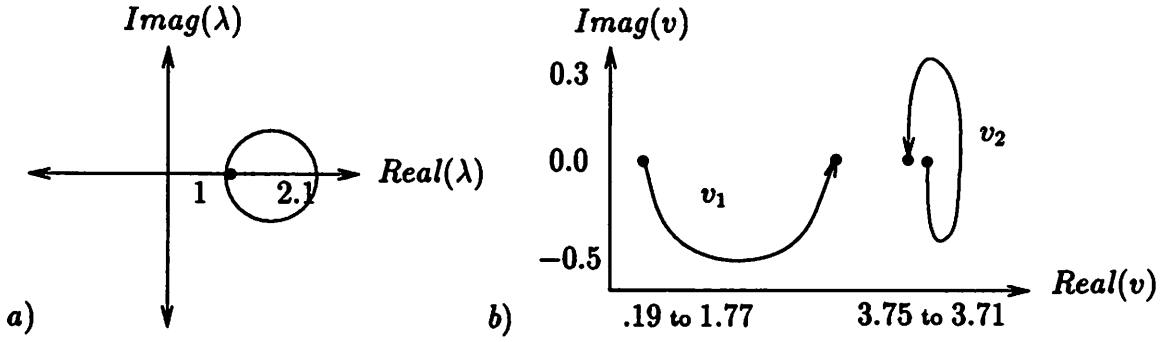

Figure 8: a)Complex orbit in parameter space. b)Complex solution trajectory from $v = (0.199, 3.754)$ to $v = (1.775, 3.707)$ around a fold.

$$\begin{aligned} Re(H_1(v_r, v_i, \lambda_r, \lambda_i)) &= 0 \\ Re(H_2(v_r, v_i, \lambda_r, \lambda_i)) &= 0 \\ Im(H_1(v_r, v_i, \lambda_r, \lambda_i)) &= 0 \\ Im(H_2(v_r, v_i, \lambda_r, \lambda_i)) &= 0 \end{aligned}$$

with v_r =Re(v) and v_i =Im(v). The new solution vector is $v = (v_r, v_i) = (v_{1r}, v_{2r}, v_{1i}, v_{2i})$.

Figure 10 shows the smooth, fold-free complex solution path from $v = (0.199, 3.754)$ to $v = (1.775, 3.707)$ obtained by tracing a full circle in parameter space around the fold point $\lambda \approx 2.1$. □

Example 2:

Simulation results on the homotopy function $H(x, \lambda) = sin(1/x) - \lambda = 0$, often used as a benchmark for fold traversal in path following algorithms, indicate that the efficiency of fold avoidance in complex space is relatively independent of fold sharpness.

The function $H(x, \lambda) = sin(1/x) - \lambda = 0$, shown in Figure 11(a), has folds of increasing sharpness at $\lambda = \pm 1$ as $x \to 0$. Setting $\lambda^* = 0$ and $r = 1.2$, the trajectory $\lambda = \lambda^* + r(1 - e^{i\theta}), \theta = 0 : 2\pi$, through complex parameter space shown in Figure 11(b) leads to a smooth, fold and bifurcation-free path in complex solution space from $x = \frac{1}{k\pi}$ to $x = \frac{1}{(k+1)\pi}$. Figure 11(c) shows a solution trajectory from $x = \frac{1}{1000\pi}$ to $x = \frac{1}{1001\pi}$.

Using a simple Newton corrector scheme, performance in complex space appeared to be independent of fold sharpness and mainly limited by machine precision. For instance, at $k = 10^2, 10^3, 10^4$, and 10^7, and with $r = 1.2$ and a step size of $\frac{2\pi r}{20}$ (20 steps around the complex parameter circle using a simple Newton corrector scheme), a single Newton iteration per step was required to trace a path from $x = \frac{1}{k\pi}$ to $x = \frac{1}{(k+1)\pi}$, with a tolerance of $1/100k$. Note that while fold sharpness greatly increases with k, the performance of this simple,

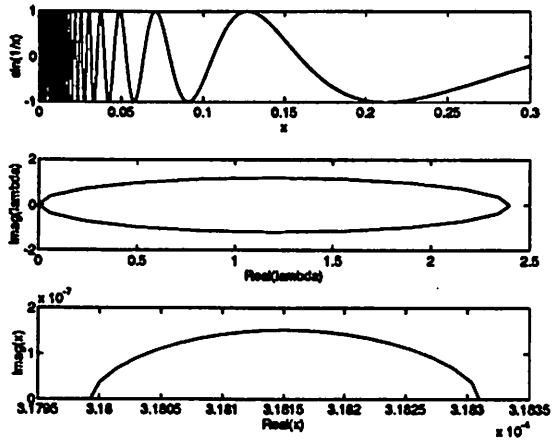

Figure 9: a) Graph of $sin(1/x)$, b) Simple closed curve traced through complex parameter space with $\lambda = 0$ as an endpoint, encircling $\lambda = 1$, c) Corresponding path through complex solution space.

fixed step-size, monotonic Newton corrector scheme did not vary. These results are in direct contrast to existing path following schemes in real space such as arclength parameterized methods and interval methods, for which efficiency greatly depends on fold sharpness. □

4 Avoiding Real Fork Bifurcations

Homotopy paths with real bifurcations are characterized by splitting paths in solution space, a nontransversal intersection of the path through parameter space with the bifurcation set, and a loss of rank of the real extended Jacobian matrix $DH_{x,\lambda} = [\partial H/\partial x, \partial H/\partial \lambda]$ at the bifurcating parameter value. An example of a real bifurcation along the solution curve of a single parameter homotopy function is the fork shown in Figure 12(b), where one real solution path bifurcates into three real solution paths. In the case of the third order polynomial example $H(x, \lambda_1, \lambda_2) = x^3 - \lambda_1 x + \lambda_2 = 0$, this forked solution could correspond to a line in parameter space passing through the midline of the bifurcation set. That is, the solution is the set of points x such that $H(x, \lambda_1, \lambda_2) = x^3 - \lambda_1 x + \lambda_2 = 0$ with $\lambda_2 \equiv 0$ and λ_1 varying from -1 to 1. We call $x^3 + x = 0$ our initial system, and $x^3 - x = 0$ our final system of interest. At $\lambda_1 = 0$ the single real solution curve hits a bifurcation point (triple root) and then splits into three real branches. Though not generic, fork bifurcations arise in circuit applications because of symmetries and ideal element modeling (see Example 3 below). They also arise when applying homotopy methods to finding periodic solutions of parameterized dynamical systems exhibiting period doubling. Period doubling, described in [16], is essentially a fork bifurcation.

A solution path corresponding to a single-parameter homotopy encountering a bifurcation point will either fail when the Jacobian $DH_{x,\lambda}$ drops rank (unlikely because of sampling and finite precision) or suffer from ill-conditioning in the neighboring region. We want to know

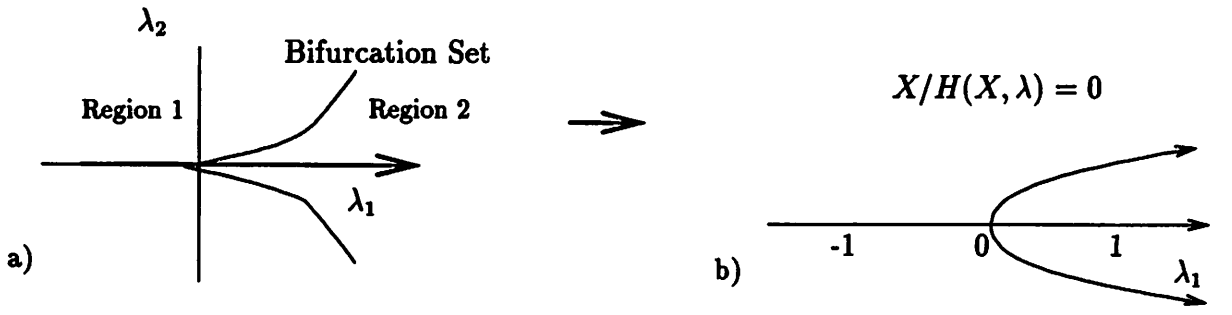

Figure 10: a) A path through real, 2-d parameter space passing through the cusp ($\lambda_1 = \lambda_2 = 0$) of the bifurcation set, given by the equation $-(\lambda_1/3)^3 + (\lambda_2/2)^2 = 0$. In Regions 1 and 2, $H(x, \lambda_1, \lambda_2) = 0$ has one and three real solutions, respectively. b) The forked real solution path of the homotopy function $H(x, \lambda_1, \lambda_2) = x^3 - \lambda_1 x + \lambda_2 = 0$ corresponding to the path through parameter space shown in a).

whether real and/or complex multi-parameter methods can avoid a fork bifurcation point, and, if so, whether all three branches will be accessible. We have found that:

Result 3: Real 2-parameter homotopy *can* be used to forge a path around the fork bifurcation point to access either outer branch without passing over a fold. Such methods, however, *cannot* be used to forge a path around the bifurcation point to access the middle branch without passing over a fold.

Result 4: Complex 2-parameter homotopy *can* be used to forge a path around the fork bifurcation point to access the middle branch without passing over a fold.

In the case of our polynomial example, Figure 13 shows the changes in solution curve topology that occur when real 2-parameter homotopy is used to bypass the triple root. Upon approaching the bifurcation point $\lambda_1 = \lambda_2 = 0$, a real half circle $(\lambda_1, \lambda_2) = (-\epsilon \cos\theta, \epsilon \, sin\theta), \epsilon > 0$ is traversed from $\theta = 0$ to $\theta = \pi$ around the bifurcation point. This has the effect of splitting the fork into a fold, and a simple curve which is traced to an outer solution branch, as shown in Figure 13(b). While either of the two outer solution branches of the fork may be reached without encountering a bifurcation point by tracing a half circle through real 2-parameter space ($\theta \geq 0$ for one, $\theta \leq 0$ for the other), the middle solution branch cannot be reached without passing over a fold.

Results in algebraic geometry can explain these observations as follows. As a class, bifurcation values corresponding to roots of multiplicity three (such as $\lambda_1 = \lambda_2 = 0$ in the real parameter plane of our polynomial $x^3 - \lambda_1 x + \lambda_2 = 0$) generally have codimension two in parameter space. This means that any perturbation of (λ_1, λ_2) away from $(0, 0)$ will take us to solutions that are not triple roots. Also, since a real bifurcation corresponds to a nontransversal intersection with the bifurcation set in parameter space, a perturbation of the

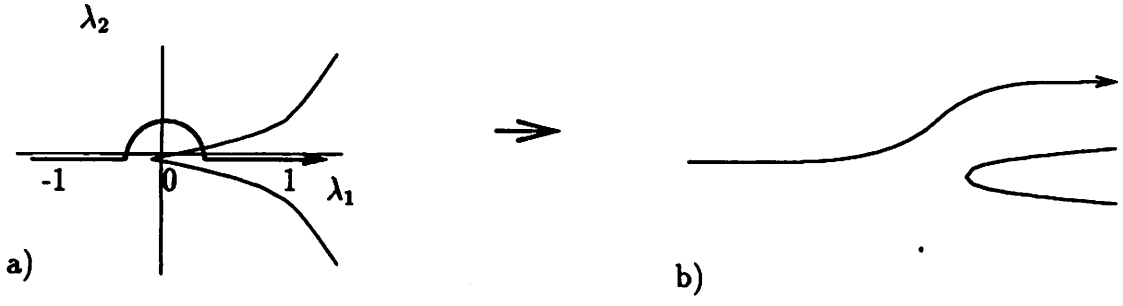

Figure 11: Real 2-parameter homotopy is used to avoid the fork bifurcation and access either outer solution branch. a) A path through the real parameter plane avoiding the bifurcation point $\lambda_1 = \lambda_2 = 0$. b) The solution topology of the function $H(x, \lambda_1, \lambda_2) = x^3 - \lambda_1 x + \lambda_2 = 0$ corresponding to the path shown in (a). Note that the fork has decomposed into a simple curve leading to an outer solution branch and a fold.

path through parameter space generally resolves the real bifurcation. Thus, we would expect a path through parameter space that avoids $(0,0)$, such as the one shown in Figure 13(a), to transversally intersect the bifurcation set, to be free of triple root values, and for the corresponding solution curve(s) to be free of real bifurcations. This expectation is borne out, as evidenced in Figure 13(b). In fact, forging a real path around the fork bifurcation point is equivalent to the classical remedy against codimension-two or higher bifurcations, that of perturbing the equations by a small amount.

However, as discussed in Section 3, bifurcation sets in real parameter space have codimension one and divide the space. The bifurcation set of $H(x, \lambda_1, \lambda_2) = x^3 - \lambda_1 x + \lambda_2 = 0$, described by the equation $-(\lambda_1/3)^3 + (\lambda_2/2)^2 = 0$ and shown in Figure 12(a), is entirely composed of generic fold values (parameter values at which H has a double root), with the exception of the triple root value $\lambda_1 = \lambda_2 = 0$. This means that although we expect that a path through real parameter space from $(\lambda_1, \lambda_2) = (-1, 0)$ to $(\lambda_1, \lambda_2) = (1, 0)$ avoiding $(\lambda_1, \lambda_2) = (0, 0)$ will not be associated with a bifurcating solution path, we do expect any such path through parameter space to include a generic fold value, and thus be associated with a fold. As seen in Figure 13(b), this fold is not a problem for the homotopy method because the solution path being followed is not the one with the fold. Notice that there are two disconnected curves, one simple and the other folded.

Bifurcation avoidance in complex parameter space is illustrated in Figure 14. Parameter λ_2 is held constant at zero, and a curve $\lambda_1 = \epsilon e^{i\theta}$ from $\theta = 0$ to $\theta = \pi$, a half circle, is traversed in the complex parameter plane. With this excursion in the complex domain, the two outer solution branches separate into the complex plane from the central real branch, as shown in Figure 14(b). Thus, a complex half-circle in parameter space will bypass the bifurcation point and lead to the center root.

To understand fork bifurcation avoidance in complex space, we introduce the concept of

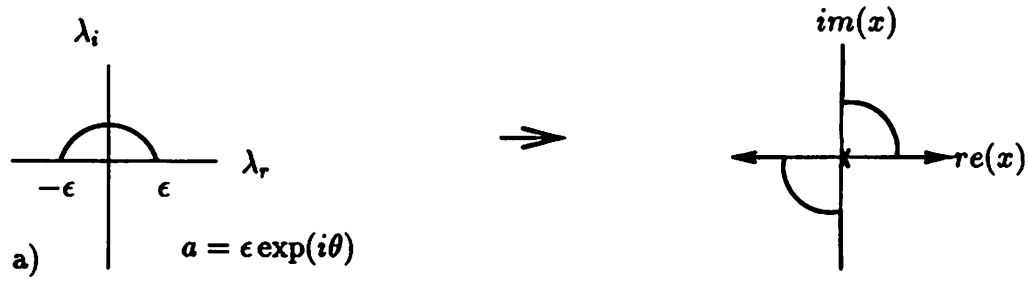

Figure 12: Complex 2-parameter homotopy is used to access the center root. a) A half-circle excursion in the complex parameter plane around the bifurcation point $\lambda = 0$. b) The root locus of $H(x, \lambda_r, \lambda_i) = x^3 + (\lambda_r + i\lambda_i)x = 0$ corresponding to the parameter path shown in a). The outer branches separate from the central branch.

reducibility [12, 11]. An equation $H(x, \lambda) = 0$ is reducible if it may be written in product form $H(x, \lambda) = P(x, \lambda)Q(x, \lambda) = 0$, so that for any value of λ, the roots of H are the union of the roots of P and Q, both analytic functions in x and λ passing through zero. Examples of analytic functions are polynomials and exponentials.

With the exception of parameter values λ for which P and Q have the same solutions, the solution set of H is composed of invariant sets. That is, a homotopy path that starts on the solution surface of P or Q, respectively, will stay there, regardless of the path taken through parameter space. As we will see in the next section, this is not true for irreducible systems of equations, for which solution surfaces are connected.

Let us now consider the path along the midline ($\lambda_2 = 0$) of the bifurcation set of the homotopy function $H(x, \lambda_1, \lambda_2) = x^3 - \lambda_1 x + \lambda_2 = 0$. Along this path this homotopy function is *reducible* and becomes $H(x, \lambda_1) = (x^2 - \lambda_1)x$, the product of complex-coefficient polynomials $P(x, \lambda_1) = x^2 - \lambda_1$ and $Q(x) = x$. At $\lambda_1 = 0$, the double root of $P(x, \lambda_1) = 0$ coincides with the single root of $Q(x)$, giving H a triple root. This junction is the fork bifurcation shown in Figure 12(b). Since H is reducible along the midline ($\lambda_2 = 0$), and the single real solution branch from $\lambda_1 < 0$ is on the same solution manifold as the central solution branch for $\lambda_1 > 0$, forging a path in complex parameter space from $\lambda_1 = -\epsilon$ to $\lambda_1 = \epsilon$ around the bifurcation point $\lambda_1 = 0$ not only pre-empts a bifurcating or folded solution path; it also eliminates the possibility of the solution curve leaving the solution set of Q. Thus, a half-circle traversal in complex parameter space must lead to the central branch.

The above conclusions also apply to irreducible homotopy functions exhibiting forked, bifurcating solution paths. To see this, consider a perturbed version of the previous example, namely $H(x, \lambda_1, \lambda_2) = x^3 - \lambda_1 x + \lambda_2$ with $\lambda_2 = \epsilon\lambda_1^2$. This homotopy function is irreducible, and has bifurcating behavior equivalent to that of the previous example. In this perturbed case, varying λ_1 from -1 to 1 amounts to following a smooth path, tangent to $\lambda_2 = 0$, through

the point (0,0) of the bifurcation set shown in Figure 12(a). The resulting behavior obtained by complexifying λ_1 is topologically identical to that obtained in the preceding example. Specifically, the real ($x = 0$) and complex ($x = \pm\sqrt{\lambda_1}$) solution branches are perturbed by a term of order $\epsilon\lambda_1$, which is an asymptotically negligible perturbation for sufficiently small ϵ and λ_1. Hence, the behavior is locally identical to that of the unperturbed homotopy. [2]

In summary, real bifurcations are characterized by a drop of rank in the extended Jacobian $DH_{x,\lambda}(x,\lambda)=[\partial H/\partial x, \partial H/\partial\lambda]$, a nontransversal intersection with the bifurcation set in parameter space, and nongenericity. When encountering a real forked bifurcation along a homotopy path as in Figure 12, real two-parameter homotopy may be used to avoid the bifurcation point and access the two outer solution branches, and complex parameter homotopy may be used to access the central solution branch without passing over a fold. Similarly, if the fork bifurcation is approached from the opposite direction, real two-parameter homotopy may be used to trace a fold- and bifurcation-free path from either outer branch to the single solution branch beyond the bifurcation point, and complex parameter homotopy may be used to trace a regular path from the central branch of the fork to the single solution branch beyond the fork bifurcation point. In all cases local ϵ half-circle excursions through parameter space signaled by a drop in the rank of the Jacobian $D_{x,\lambda}H$ are sufficient to accomplish this avoidance. Though scalar equations were used to develop the reasoning supporting these results, the application of Lyapunov-Schmidt reduction (as mentioned in the previous section and summarized in Appendix A) ensures that the reasoning applies to multivariate systems of equations as well, such as those describing nonlinear circuits. We now present a simple circuit example.

Circuit Example 3 (Flip-Flop):

The flip-flop of Figure 15 has a bifurcation that is topologically identical to the fork described above when voltage source continuation is used to find DC operating points [6]. We take the real 2-parameter homotopy function

$$\begin{aligned} H_1(v,\lambda) &= (vc_1 - \lambda_1 V_{CC})/RC + (vc_1 - vb_2)/RB + \hat{ic}_1(vb_1, vc_1) \\ H_2(v,\lambda) &= (vb_1 - vc_2)/RB + \hat{ib}_1(vb_1, vc_1) \\ H_3(v,\lambda) &= (vc_2 - \lambda_2 V_{CC})/RC + (vc_2 - vb_1)/RB + \hat{ic}_2(vb_2, vc_2) \end{aligned}$$

[2]Reference [9] contains a scheme equivalent to the half circle in complex parameter space that we have prescribed for accessing center solution branches of real forked bifurcations. The authors of [9] suggest that such a scheme is appropriate for avoiding all types of singular points, an assertion that is problematic if one is interested in real solution curves only, or in tracing all solution curves. If the singular point encountered corresponds to an ordinary branch point, but not to a real bifurcation, a half-circle excursion in complex parameter space will result in a trajectory leading to a complex solution curve. For example, if one takes the polynomial $H(x,\lambda_2) = x^3 + \lambda_2 = 0$ and traces a path through parameter space along the λ_2 axis, the singular point at $\lambda_2 = 0$ now corresponds to an ordinary triple root, rather than to a fork bifurcation. A half-circle excursion in the complex plane around the singular point $\lambda_2 = 0$ will take the solution to a complex branch $x = |\lambda_2|^{1/3} e^{i2\pi/3}$. In this case a 3π rotation is required to bypass the triple root and return to a real solution curve.

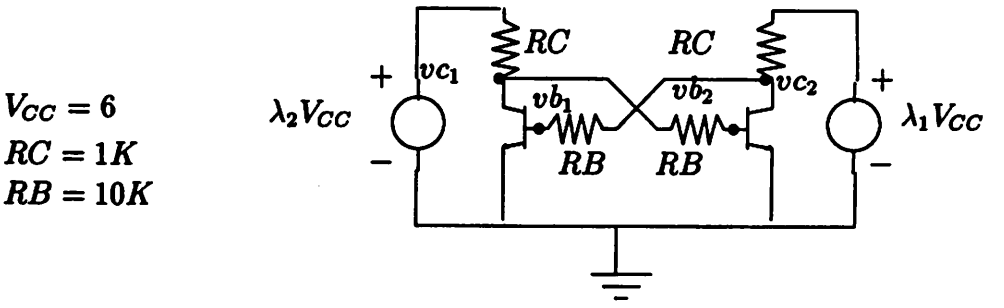

Figure 13: Flip-flop circuit diagram.

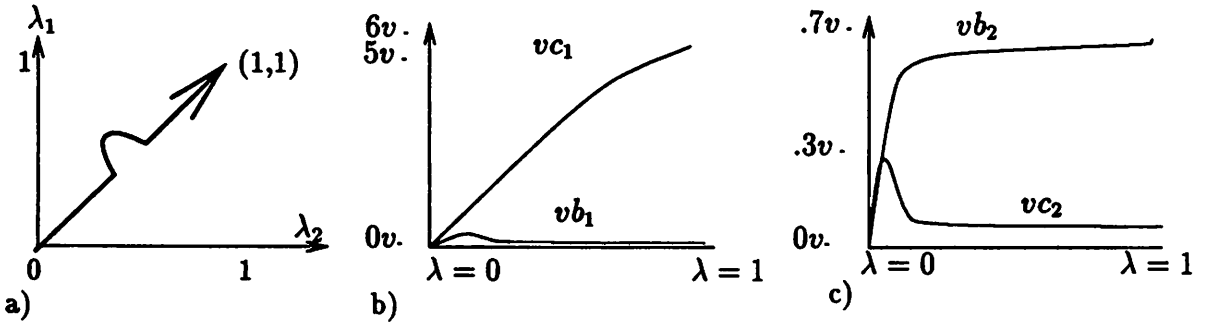

Figure 14: Real two-parameter homotopy is used to access outer solution branches. a) A curve through the real parameter plane avoiding the bifurcation point $\lambda_1 = \lambda_2 \approx .1135$. b,c) Corresponding solution curves to stable points.

$$H_4(v, \lambda) \;=\; (vb_2 - vc_1)/RB + \hat{ib}_2(vb_2, vc_2)$$

where $\hat{ic}_i = I_s(e^{vb_i/v_t} - 1) - I_s/a_r(e^{(vb_i - vc_i)/v_t} - 1)$, $\hat{ib}_i = -\hat{ic}_i - (-I_s/a_f(e^{vb_i/v_t} - 1) + I_s(e^{(vb_i - vc_i)/v_t} - 1))$, $a_f = 0.945$, $I_s = 10^{-14}$, $v_t = 0.025v$, $a_r = 0.65$, and with node voltages $v = (vc_1, vb_1, vc_2, vb_2)$ and parameters $\lambda = (\lambda_1, \lambda_2)$. This function was obtained from the single-parameter voltage continuation in [6] by converting λ in the first and third equations, which multiply the voltage source, into two independent variables.

Figures 16(b,c) show the solution trajectory obtained by tracing a clockwise half-circle path in the real parameter plane around the bifurcation point $\lambda_1 = \lambda_2 \approx .1135$, shown in Figure 16(a). As discussed in the polynomial example, a stable solution is accessed and the bifurcation point is avoided. Because of symmetry, a counterclockwise half-encirclement of the bifurcation point leads to the other stable circuit solution.

A complex 2-parameter homotopy function may be obtained from the same single-

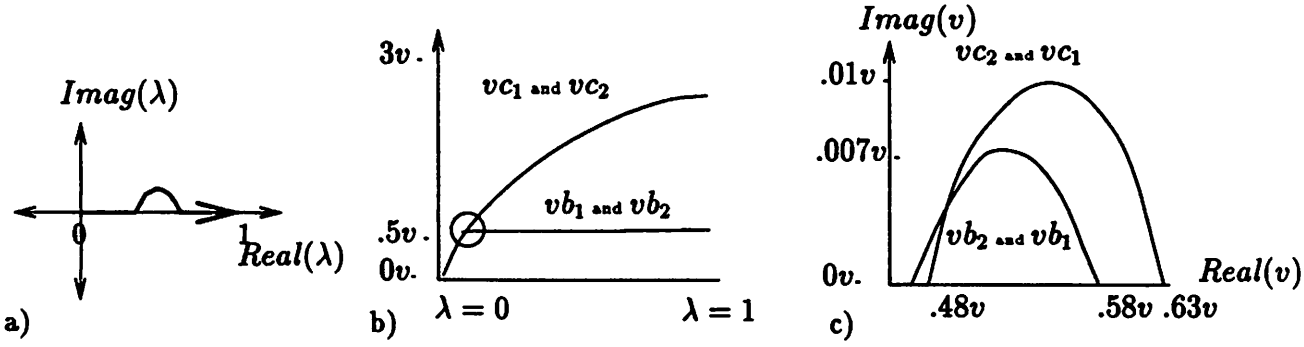

Figure 15: Complex two-parameter homotopy is used to access the central, metastable solution branch ($\lambda_1 = \lambda_2 = \lambda_r + i\lambda_i$). a) Path through complex parameter space avoiding the bifurcation point. b) Associated solution paths to the metastable branch, real except for region inside of circle. c) A blow up of the complex solution path around the bifurcation point (blow up of circle shown in (b)).

parameter homotopy function by letting λ be complex in the above equations ($\lambda_1 = \lambda_2 = \lambda_r + i\lambda_i$). Figures 17(b,c) show the bifurcation-free solution trajectories obtained by a half-circle excursion in complex parameter space (Figure 17(a)). Figure 17(c) shows a blow-up of the excursion in the complex domain. As expected, the central, metastable solution is accessed at the end of a bifurcation-free path. □

5 Finding Multiple Solutions

Homotopy methods have been applied to the task of finding multiple dc solutions of nonlinear circuits, a potentially valuable feature of a circuit simulation program. Most

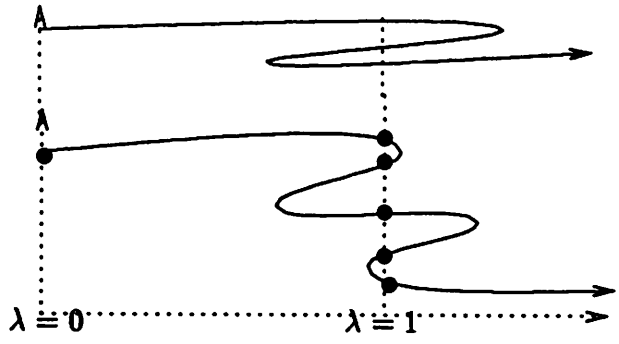

Figure 16: Extended curve following. Illustration of disconnected solution branches.

continuous, single-parameter homotopy methods for finding multiple solutions of nonlinear circuits take either a multiple starting point or an extended curve following approach. The multiple starting point approaches involve choosing a number of points to serve as initial values of continuation paths, corresponding either to an 'easy' starter system with multiple solutions, or to numerous starter systems with different, unique solutions. In either case, all the paths are then followed to circuit solutions at $\lambda = 1$. Since for some homotopies, paths may diverge to infinity, meet at a fold or at a bifurcation point, or lead to the same solution, these methods may not find all real solutions, and can be inefficient.

The extended curve-following approach, also called Lambda Threading [4, 5, 6], follows a single solution path past $\lambda = 1$ in the hope that the curve will reverse direction and pass through $\lambda = 1$ multiple times. This method may fail to find all solutions if the path followed does not pass through all solution points [5], as illustrated in Figure 18. For example, the single parameter homotopy function in Example 1 (the tunnel diode circuit) produces solution curves that pass through a number of solution points that depend on the starting point v_0. Though the solution curve beginning at $v_0 = (v_1, v_2) = (3, 0)$ passes through all nine solutions [5], Figure 9 shows a curve, stemming from $v_0 = (0, 0)$, that passes through only five solutions.

We focus on multi-parameter versions of the extended curve following approach. We address the question of whether adding extra homotopy parameters opens up the possibility of finding all solutions of an arbitrary circuit. Since a fundamental problem with the extended curve following approach is the presence of real disconnected solution branches, we are interested in the potential of multi-parameter methods for joining disjoint branches. That is, given a real, single parameter homotopy function with disconnected solution branches, can adding or complexifying parameters result in a completely connected solution manifold that, in principle, can be navigated from solution point to solution point until all circuit solutions are found? Also of interest, if solution surface connectivity results are to lead to practical algorithms, is how these paths might be traced.

This section concentrates on complex parameter homotopy as applied to the extended curve following approach. Essential to this discussion is the notion of an irreducible analytic homotopy function, and its complex solution structure [11, 12]. As previously discussed, an analytic equation $H(x, \lambda) = 0$ is *reducible* if it may be written in product form $H(x, \lambda) = P(x, \lambda)Q(x, \lambda) = 0$, so that the roots of H are the union of the roots of P and Q, both analytic functions in x and λ passing through zero. The equation $H(x, \lambda) = 0$ is *irreducible* if it is not reducible, and a system of equations $H(x, \lambda) = 0$, $H : C^n \times C \rightarrow C^n$, is irreducible if each h_i is irreducible, where $H = [h_1, h_2, ..h_n]'$. For example, $x_1^2 - x_2^2\lambda = 0$ is irreducible, as is $e^{-x_1}(a_0 + a_1x_1 + a_2x_2 + .. + a_nx_n) = 0$, because the former function does not factor into the product of two analytic functions, while the latter function only factors into the product of a polynomial and an exponential, an analytic function which does not pass through zero called a *unit*. However, the solution set of $x_1^4 - x_2^2\lambda^2 = 0$ reduces to the product of the solution sets of $x_1^2 - x_2\lambda = 0$ and $x_1^2 + x_2\lambda = 0$.

Appendix B details the statement and proof of the following proposition of [12, p21].

Proposition: An analytic variety V is irreducible if and only if V^* is connected, where V^*

is the locus of smooth points of V.

Simply put, the proposition indicates that the *complex solution set* of an irreducible system of equations $H(x,\lambda) = 0$, $H : C^n \times C \rightarrow C^n$, which takes the form of a number of surfaces above a neighborhood of each regular point λ, is *connected* over the complex parameter plane. This means that given an irreducible, analytic homotopy function H with a complex parameter λ, there exist regular paths through the complex parameter plane connecting any solution x_1 of $H(x,\lambda') = 0$ to any other solution x_2 of $H(x,\lambda') = 0$, provided λ' is a regular parameter value. A consequence of this solution manifold connectivity, in conjunction with the codimension two bifurcation sets in complex parameter space, as discussed in Section 3, is that complex parameter homotopy methods have the potential for finding all solutions of nonlinear circuits via regular paths. We list this consequence in the following result.

Result 5: Complex parameter homotopy methods can, in principle, find all solutions of a circuit modeled by analytic functions, without passing through folds or singular points.

Because exponential, sinusoidal and polynomial equations are all analytic, the class of circuits that Result 5 applies to is large, allowing for many standard diode and transistor models. An obvious question is how easy or difficult it is to design an irreducible homotopy function. While in general it may be difficult to determine whether an arbitrary multi-variate function is irreducible, it is significantly more straightforward to deliberately design an irreducible embedding. For example, given any function $f(x) = 0$, $f : C^n \rightarrow C$, either reducible or irreducible, the embedding $h(x,\lambda) = f(x) + \lambda$ is an irreducible homotopy function. And with some thought, many other irreducible homotopy functions can be designed as well.

To summarize this section so far, assume that the dc operating points are defined as being the real solutions of the analytic circuit equations

$$F(x) = \bar{0} \tag{6}$$

where $F : C^n \rightarrow C^n$. Then the homotopy function

$$H(x,\lambda) = \bar{0},\ H : C^n \times C \rightarrow C^n, \tag{7}$$

with each $h_i(x,\lambda)$ irreducible and $H(x,\lambda^*) = F(x)$ at some $\lambda^* \in C$ has a complex solution space that regularly connects all dc operating points.

Now that results from algebraic geometry have been invoked to establish that solution manifolds are regularly connected in complex space, and thus are navigable from solution surface to solution surface, we move on to explore the nature of this connectivity and how it might be exploited to join real disjoint solution branches and to find multiple circuit solutions. We revisit the third order polynomial $H(x,\lambda_1,\lambda_2) = x^3 - \lambda_1 x + \lambda_2 = 0$ discussed in Section 4 to illustrate the nature of solution-surface connectivity, and to provide an example of complex solution paths joining real disjoint solution branches.

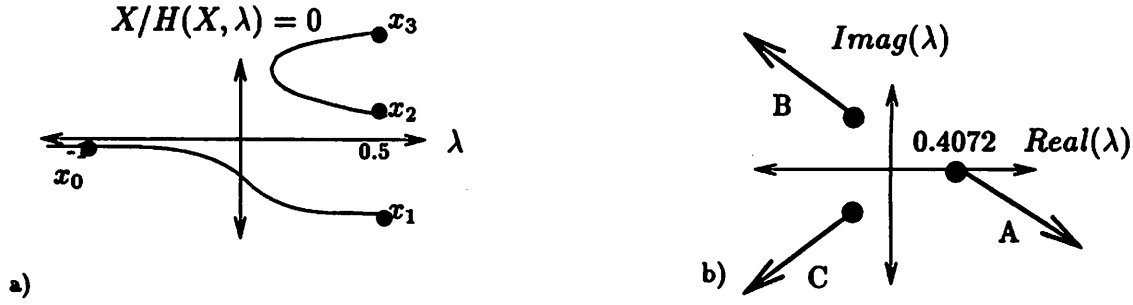

Figure 17: a) The solution topology of the function $H(x,\lambda) = x^3 - \lambda x + .1 = 0$. Note disconnected paths. b) The three finite branch points of $H(x,\lambda) = x^3 - \lambda x + .1 = 0$, evenly distributed on a circle of radius 0.4072, and branch cuts A,B and C.

Complex Solution Surface Connectivity: Joining Real Disjoint Solution Branches The polynomial $H(x,\lambda) = x^3 - \lambda x + b$, with real, fixed, non-zero b, is a simple example of an irreducible homotopy function with disjoint solution branches. As shown in Figure 19(a), the homotopy function $H(x,\lambda) = x^3 - \lambda x + .1 = 0$ ($b = .1$ for the remainder of the discussion) has two real disconnected branches, a simple curve and a fold. If one were interested in finding all solutions of $H(x, 0.5) = 0$ from the real solution of $H(x,-1) = 0$, $x_0 = -0.099$, using real extended curve following, one would come to the erroneous conclusion that $H(x, 0.5) = 0$ has a single real solution at $x_1 = -0.791$. However, Result 5 indicates that there exist paths through complex parameter space that regularly join the two real, disconnected branches.

In fact, if after finding the solution $x_1 = -0.791$ we make λ complex and trace a full circle in complex parameter space starting from $\lambda = 0.5$, with center $\lambda = 0.5 - r$ and a radius $r \geq 0.45$ (shown in Figure 22(e)), the corresponding complex solution trajectory (shown in Figure 22(f)) follows a path from $x_1 = -0.791$ to a solution residing on the folded, disconnected branch, $x_3 = 0.569$. From there, the solution $x_2 = 0.222$ may be easily found, either by following the real folded solution path or by performing another complex-parameter branch point encirclement. That way, all three solutions are found instead of just the one on the simple, disconnected branch.

Solution manifold connectivity, for this example and for any parameterized analytic system of equations, can be understood in terms of the existence and positioning of branch points and branch cuts. A regular point λ has a neighborhood, above which, the solution structure takes the form of a set of manifolds. A branch point is a parameter value $\lambda \in C$ at which a complex-parameter homotopy function $H(x,\lambda) = 0$ has repeated roots. As such, the branch points correspond to parameter values where one or more solution manifolds contact each other. In our polynomial example $H(x,\lambda) = x^3 - \lambda x + .1 = 0$, there are three manifolds above each regular point, and four parameter values corresponding to repeated roots: $\lambda = 0.4072$, $\lambda = 0.4072e^{i2\pi/3}$, $\lambda = 0.4072e^{i4\pi/3}$, and $\lambda = \infty$. The three finite branch points, shown in Figure 19(b) and superimposed on the complex parameter paths illustrated

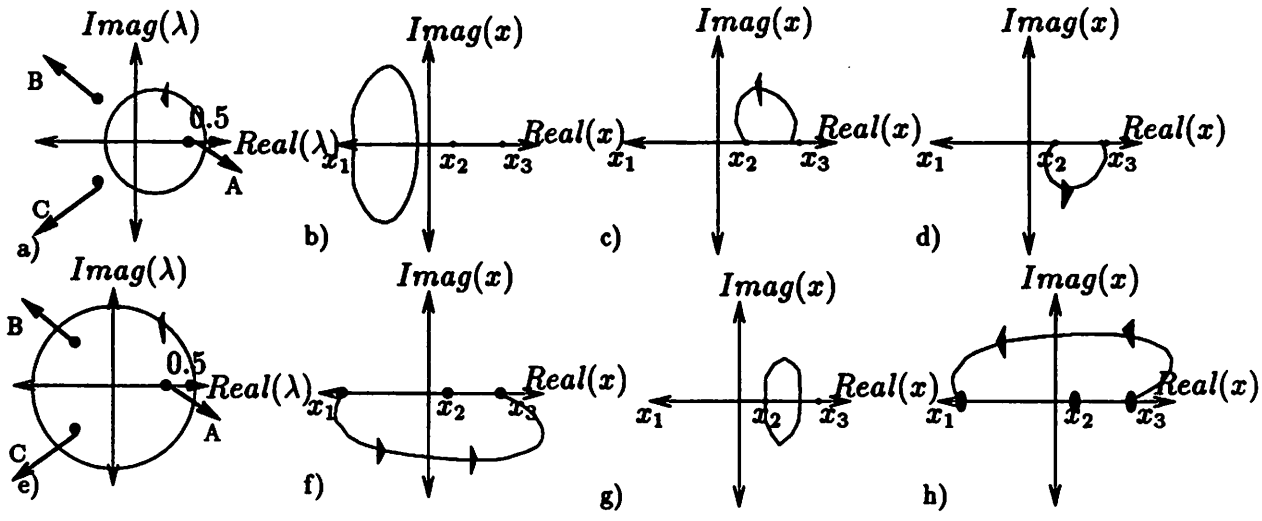

Figure 18: a) Revolution in the complex parameter plane encircling one branch point and passing through branch cut A. b) Closed solution trajectory from x_1 corresponding to path in (a). c) Solution trajectory from x_3 to x_2 corresponding to path in (a). d) Solution trajectory from x_2 to x_3 corresponding to path in (a). e) Revolution in the complex parameter plane encircling three branch points. f) Solution trajectory from x_1 to x_3 corresponding to path in (e). g) Closed solution trajectory from x_2 corresponding to path in (e). h) Solution trajectory from x_3 to x_1 corresponding to path in (e).

in Figure 22, were derived by solving the simultaneous constraints $H(x, \lambda) = 0$ and the repeated root condition $D_x H(x, \lambda) = 0$, for λ. They correspond to double roots of $H(x, \lambda) = 0$. Each of these three finite branch points locally connects two of the three solution manifolds in such a way that tracing a small closed curve through complex parameter space around a single branch point will result in a solution trajectory from one manifold to another. For example, a closed path around the branch point $\lambda = 0.4072$ with $\lambda = 0.5$ as a starting point, as shown in Figure 22(a), traces a solution path from x_2 to x_3, or vice-versa, as shown in Figures 22 (c,d).

Now that branch points have been explained and identified for our polynomial example, we move on to branch cuts. A branch cut is a nonunique curve through parameter space with finite or infinite branch points at the endpoints, symbolizing a connection between solution manifolds. Branch cuts for our polynomial example are shown in Figure 19(b), and superimposed on Figure 22(a,e). Assuming that the solution point x_1 is locally identified with solution surface 1, and that solutions x_2 and x_3 are locally identified with solution surfaces 2 and 3, respectively, branch cut A connects surface 2 to surface 3, branch cut B connects surface 1 to surface 2, and branch cut C connects surface 1 to surface 3. Each is a ray connecting a finite branch point to the infinite branch point.

The location of branch points and branch cuts determine solution surface connectivity, and thus the set of paths that will connect a solution of $H(x, \lambda') = 0$ (λ' fixed) to any other solution of $H(x, \lambda') = 0$. One way of thinking about (and keeping track of) the movement of a solution path from solution manifold to solution manifold as the complex parameter is varied, is as a sequence of permutations in the ordering of solution manifolds, signaled by branch cut crossings. For example, a simple closed curve in complex parameter *space* through branch cut A, as shown in Figure 22(a), will result in a change of solution ordering, from $(1,2,3)$ to $(1,3,2)$, because A joins surfaces 2 and 3. As shown in Figures 22(c,d), the corresponding solution path starting at x_2 will lead to x_3, while one starting at x_3 will lead to x_2. If a solution path were started at x_1, it would stay on surface 1 and not lead to a new solution, because no branch cut connecting solution surface 1 to another solution surface was crossed.

Similarly, a simple closed path in complex parameter space encircling all three finite branch points and crossing all three branch cuts, like the one shown in Figure 22e, permutes the solution surface ordering from $(1,2,3)$ to $(2,1,3)$ to $(2,3,1)$ to $(3,2,1)$, because branch cuts B, C, and then A are crossed. The net permutation is from $(1,2,3)$ to $(3,2,1)$ (with corresponding solution paths from (x_1, x_2, x_3) to (x_3, x_2, x_1)). Such a path through parameter space will lead from solution x_1 to x_3, or from x_3 to x_1, but cannot lead to a new solution if x_2 is a starting value, as illustrated in Figures 22 f,g,h. Associated solution paths for any other curve through the complex parameter plane may be analogously predicted, given our knowledge of the the existence and positioning of branch points and branch cuts for this example.

Next, we present a branch point encirclement experiment on the tunnel diode circuit in Example 1 with nine real solutions, only five of which are accessible using ordinary extended curve following from the starting value $v_0 = (0,0)$.

Circuit Example 4 (Tunnel Diode Circuit Revisited):

A simple algorithm that involves tracing non-infinitesimal closed curves in complex parameter space with $\lambda = 1$ as an endpoint was found capable of finding all circuit solutions efficiently on several examples, even from solution branches of homotopy functions that do not pass through all solution points (disjoint branches as in Figure 18). To illustrate, we return to the tunnel diode circuit in Example 1 and step through the procedure.

First, we traced the real solution curve of $H(v, \lambda) = 0$ from $v_0 = (v_1, v_2) = (0,0)$ at $\lambda = 0$ to a solution of the circuit, $v = (0.228, 0.827)$ at $\lambda = 1$. Instead of continuing along the real solution curve to find the next solution, as one would in a real, single-parameter extended curve following algorithm [5], we made λ complex and traced a full circle in complex parameter space starting from $\lambda = 1$, with center $\lambda = 1 + r_1$ and radius r_1 (see Figure 23(a)). If the circle traversed intersects a branch cut and contains a branch point, the revolution in complex parameter space can result in a fold-free solution path from the initial solution $v = (0.228, 0.827)$ to another circuit solution. For instance, $v = (0.219, 1.673)$ is reached

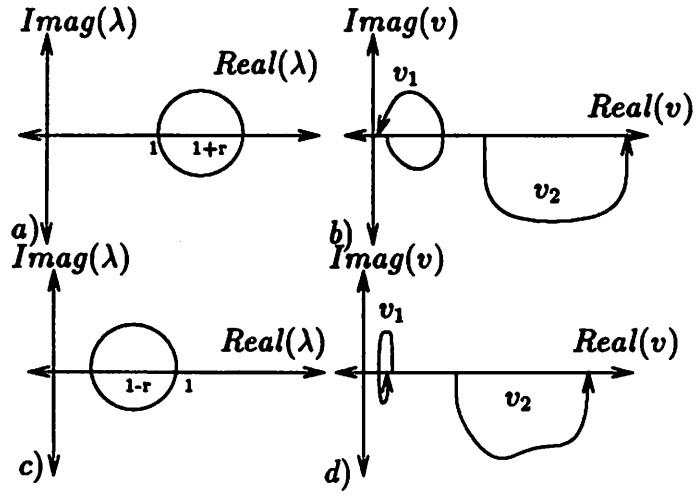

Figure 19: a) First revolution in complex parameter space. b) Corresponding solution trajectory from $v = (0.228, 0.827)$ to $v = (0.219, 1.673)$. c) Second revolution in complex parameter space. d) Corresponding solution trajectory from $v = (0.219, 1.673)$ to $v = (0.199, 3.754)$.

when a circle of radius $r_1 = 0.2$ is traversed in complex parameter space. The corresponding solution trajectory is shown in Figure 23(b).

To find yet another solution, we traced a circle in complex parameter space starting at $\lambda = 1$ with center $\lambda = 1 - r_2$ (see Figure 23(c)), and followed a curve from the second solution $v = (0.219, 1.673)$ to a third solution $v = (0.199, 3.754)$ ($r_2 = 0.25$). Continuing in this manner, from solution to solution, alternating the center of parameter revolution between $1+r$ and $1-r$, we were able to find all solutions of the circuit, even though we used a homotopy function with a real solution curve passing through only five solutions. With the simplest of schemes - no predictor and only a Newton corrector - we calculated each of the nine solutions (except the first) in under 15 steps (as opposed to hundreds), with an average of two corrector iterations per step. □

This example suggests that the complex solution surface connectivity discussed in this section could prove useful for connecting real disjoint solution branches and efficiently finding all solutions of nonlinear circuits. A topic for future study is that of developing ways of exploiting this global connectivity property in complex space, for example by designing homotopy functions that force all circuit solutions to be locally connected in a single algebraic element.

6 Conclusion/Summary

In this paper we introduced real and complex multi-parameter homotopy methods for solving nonlinear circuits, and explored their potential for avoiding folds and bifurcations along solution paths, and for finding multiple solutions. Generic folds, we learned, are real double roots occuring at generic fold values. We showed, using arguments from algebraic geometry, that in general no number of added real parameters can lead to fold avoidance, but that generic folds may be efficiently avoided by complexifying the homotopy parameter and tracing a closed curve in complex parameter space around the the critical fold value.

Real bifurcations are characterized by a drop of rank in the extended Jacobian $DH_{x,\lambda}$ and nongenericity. When encountering a real forked bifurcation along a homotopy path, real 2-parameter homotopy was shown to be useful in avoiding the bifurcation point and accessing the two outer solution branches, while complex parameter homotopy was shown capable of accessing the central solution branch without passing over a fold. Local ϵ half-circle excursions through parameter space (signaled by a drop in the rank of the Jacobian $D_{x,\lambda}H$) were found sufficient to accomplish this avoidance.

We also explored the potential of complex parameter homotopy methods for finding all circuit solutions, and found that in principle, at least, such methods have the potential for finding all solutions. This potential exists because complex solution manifolds are connected over the complex parameter plane. That is, given an irreducible, analytic homotopy function H with a complex parameter λ, there exist regular paths through the complex parameter plane connecting any solution of $H(x,\lambda')=0$ to any other solution of $H(x,\lambda')=0$. Solution manifold connectivity was explained in terms of the location of branch points and branch cuts. All solutions of two example systems, a circuit and a polynomial, were found efficiently using branch point encirclement from homotopy functions with real disconnected branches. Though a path through parameter space leading from one solution surface to another must encircle a branch point and intersect a branch cut, the location of which are generally not known apriori, experiments suggest that complex solution surface connectivity could prove useful in connecting real disjoint solution branches and/or efficiently finding all solutions of nontrivial circuits. Our future work plans include exploiting this global connectivity property in complex space by designing homotopy functions that force all circuit solutions to be locally connected in a single algebraic element.

A Lyapunov-Schmidt Reduction

Assume we are given a function $H : \Re^m \times \Re^k \rightarrow \Re^m$,

$$H(x,\lambda)=0, \tag{8}$$

with a bifurcation at the point (x_0,λ_0), and an associated drop of rank in the Jacobian $D_xH(x_0,\lambda_0)$ at the bifurcation point. The goal is to find a simple way of locally characterizing and studying this bifurcation. One way of doing this is the method of Lyapunov-Schmidt

[13], which involves changing coordinates in the neighborhood of the bifurcation point and reducing the problem of locally representing a bifurcation to its smallest dimension. The dimension is that of the null space of the Jacobian of H with respect to x at the bifurcation point, $D_x H(x_0, \lambda_0)$.

The idea behind this method, described in detail in [13] and the references therein, is to create nonsingular matrices $[P_u : U]$ and $[P_v : V]$, where $U, V \in \Re^{m \times p}$, and p is the rank deficit of the Jacobian $D_x H(x_0, \lambda_0)$. The matrix U consists of basis vectors for the null space of $D_x H(x_0, \lambda_0)$, so $D_x H(x_0, \lambda_0) U = 0$. The matrix V is chosen so that $V^\top D_x H(x_0, \lambda_0) = 0$. The matrix $P_v^\top D_x H(x_0, \lambda_0) P_u$ is nonsingular. Then (10) may be decomposed into

$$P_v^\top H(x, \lambda) = 0 \tag{9}$$

and

$$V^\top H(x, \lambda) = 0, \tag{10}$$

and $x \in \Re^m$ may be represented by $x = P_u w + U q$, with $w \in \Re^{m-p}$ and $q \in \Re^p$. Notice that the solution vector x has been decomposed into two parts, one in the null space of $D_x H(x_0, \lambda_0)$, and one in the range space of $D_x H(x_0, \lambda_0)^\top$.

With this change in coordinates, equations (11) and (12) become

$$P_v^\top H(P_u w + U q, \lambda) = 0 \tag{11}$$

$$V^\top H(P_u w + U q, \lambda) = 0 \tag{12}$$

and if w_0 and q_0 are chosen so that $x_0 = P_u w_0 + U q_0$, then the Implicit Function Theorem may be applied to equation (13) in the neighborhood of the bifurcation point (w_0, q_0, λ_0) to get the function $w^*(q, \lambda)$, where $w_0 = w^*(q_0, \lambda_0)$. This function, when substituted in equation (14), leads to the definition of a *bifurcation function*

$$N(q, \lambda) = V^\top H(P_u w^*(q, \lambda) + U q, \lambda) = 0 \tag{13}$$

of p equations in p unknowns characterized by $N(q_0, \lambda_0) = 0$ and $D_q N(q_0, \lambda_0) = 0$. This function locally characterizes the bifurcation. Since this paper is concerned with bifurcations at which the Jacobian $D_x H(x_0, \lambda_0)$ drops rank exactly once, $p = 1$, the bifurcation function consists of a single parameterized equation. Thus, in this case it suffices to study a univariate parameterized equation that captures the qualitative features of a bifurcation, even though the circuit equations of interest are multi-variate.

B Global Connectivity Property of Analytic Varieties

Analytic Hypersurface: V is called an *analytic hypersurface* if V is locally the zero locus of a single nonzero analytic function f.

Analytic Variety: A subset V of an open set $U \subset C^n$ is an *analytic variety* in U if, for any $p \in U$, there exists a neighborhood U' of p in U such that $V \cap U'$ is the common zero locus of a finite collection of analytic functions $f_1, \ldots f_k$ on U'.

Irreducible Analytic Variety: An analytic variety $V \subseteq U \subset C^n$ is said to be *irreducible* if V cannot be written as the union of two analytic varieties $V_1, V_2 \subset U$ with $V_1, V_2 \neq V$.

The above definitions can be found on page 12 of [12]. The following proposition may be found on page 21 of [12], along with a proof for the case of a single analytic function, outlined below. A more general proof may be found in the references cited within [12].

Proposition: An analytic variety V is irreducible if and only if V^* is connected.

In the above proposition V^* is the locus of smooth points of V, meaning that the singular locus V_s has been removed from V ($V^* = V - V_s$).

Outline of Proof:

$\Rightarrow$ (if V is reducible then V^* is disconnected)

If V is reducible, then it is the sum of distinct analytic varieties, meaning $V = V_1 \cup V_2$, with $V_1, V_2 \subsetneq V$. Note that any overlap between V_1 and V_2 will correspond to repeated roots of analytic equations, and thus will belong to the singular set of V ($(V_1 \cap V_2) \subset V_s$). Since V^* is the set V minus the singular set V_s, and any overlap between V_1 and V_2 is part of this singular set, V^* is disconnected.

$\Leftarrow$ (if V^* is disconnected then V is reducible)

1. Assume V^* disconnected, with $\{V_i\}$ connected components.
2. Take closure of each connected component, $\overline{V}_i$. The goal is to show that $\overline{V}_i$ is an analytic variety.
3. Use Weierstrass polynomials [12] to prove that $\overline{V}_i$ is the zero set of the analytic function $f_i(z) = z_n^k + \sigma_1(z')z_n^{k-1} + .. + \sigma_k(z'), z' \in C^{n-1}, \sigma_i(0) = 0$. This proves that each $\overline{V}_i$ is an analytic variety, and thus V is reducible.

Consequence of Proposition:

The proposition states that irreducible analytic varieties are regularly connected. The complex solution set of a parameterized set of analytic equations is an analytic variety. An example of such a variety is the complex solution set of parameterized circuit equations, where the circuit elements are modeled exclusively by analytic functions like linear elements, polynomials, and exponentials, and the parameter(s) also appear analytically.

If the parameterized circuit equations are irreducible, then the complex solution space is connected. This means that if one designs a homotopy function for finding dc operating points of a circuit that is both analytic and irreducible, then the solution space will be connected, and in principle one can trace regular paths from circuit solution to circuit solution, until all operating points are found.

References

[1] K. Kundert, J. White, A. Sangiovanni-Vincentelli, *Steady-State Methods for Simulating Analog and Microwave Circuits*, 1990.

[2] A. Morgan. *Solving Polynomial Systems Using Continuation for Engineering and Scientific Problems.* Prentice-Hall, Englewood Cliffs, NJ, 1987.

[3] E. Allgower, K Georg. *Numerical continuation methods: an introduction.* Springer-Verlag, 1990.

[4] Lj. Trajkoric, R. C. Melville, and S.C.Fang. *Finding DC operating points of transistor circuits using homotopy methods*, IEEE Int. Symp on Circuits and Systems, Singapore, June,1991, pp758-761.

[5] L. O. Chua and A. Ushida. *A switching-parameter algorithm for finding multiple solutions of nonlinear resistive circuits*, Int. j. cir. theor. appl., 4, 215-239, 1976.

[6] R.C. Melville, L. Trajkovic, S-C Fang and L.T. Watson. *Globally Convergent Methods for the DC Operating Point Problem*, TR 90-61, C.S. Dept., Virginia Polytechnic Institute and State University, 1990.

[7] R.C. Melville, L. Trajkovic, S-C Fang and L.T. Watson. *Artificial Parameter Homotopy Methods for the DC Operating Point Problem*, IEEE Trans on Computer-Aided Design of Integrated Circuits and Systems, June, 1993, V12 N6:861-877.

[8] L.T. Watson. *Globally convergent homotopy methods: a tutorial*, Appl. Math. and Comp., vol. 31, pp. 369-396, May 1989.

[9] R. Kalaba and L. Tesfatsion. *Solving nonlinear equations by adaptive homotopy continuation*, Appl. Math. and Comp., vol. 41, pp. 99-115, Jan 1991.

[10] E. Hille, *Analytic function theory.* Vols. I,II. Boston, Ginn, [1959-1962].

[11] K. Knopp, *Theory of functions.* Vol II. New York, Dover publications, [1945-47].

[12] P. Griffiths, J. Harris, *Principles of algebraic geometry*, New York, Wiley, 1978.

[13] S. Sastry, C. Desoer, *Jump Behavior of Circuits and Systems*, IEEE Trans on Circuits and Systems, Vol. CAS-28, No. 12, December, 1981, pp1109-1124.

[14] I. Stewart *Elementary catastrophe theory*, IEEE trans. Circuits and Systems, August, 1983.

[15] V.I. Arnold, *Catastrophe theory*, Springer-Verlag, 1984, 1986.

[16] R.L. Devaney, *An Introduction to Chaotic Dynamical Systems*, Benjamin/Cummings, 1986.

[17] D.M. Wolf and S.R. Sanders. *Multi-Parameter Methods for Finding DC Operating Points of Nonlinear Circuits* IEEE Int. Symp on Circuits and Systems, Chicago, May, 1993.

[18] A. Ushida and L.O. Chua, *Tracing solution curves of nonlinear equations with sharp turning points*, Int. J. of Circuit Theory and Applications, Vol 12, pp.1-21, 1984.

[19] J. Guckenheimer and P. Holmes, *Nonlinear Oscillations,Dynamical Systems, and Bifurcations of Vector Fields*, Springer Verlag, 1983.

[20] M. Golubitsky, D. Schaeffer. [1979a]. A theory for imperfect bifurcation via singularity theory. Comm. Pure Appl. Math,., 32, 21-98

[21] M. Golubitsky, D. Schaeffer. [1979b]. Imperfect bifurcation in the presence of symmetry. Comm. Math. Phys., 67, 205-232.